Heterogeneous ECE Processes at Channel Electrodes: Voltammetric Waveshape Theory. Application to the Reduction of Nitromethane at Platinum Electrodes

Peter B. Mills, W. Joanne Aixill, Francisco Prieto, John A. Alden, and Richard G. Compton*

Physical and Theoretical Chemistry Laboratory, Oxford University, South Parks Road, Oxford OX1 3QZ, United Kingdom

Manuela Rueda

Department of Physical Chemistry, Faculty of Pharmacy, University of Sevilla 41012 Sevilla, Spain

Received: April 3, 1998; In Final Form: June 10, 1998

Theory is developed for heterogeneous ECE reactions occurring at channel electrode that predicts the voltammetric waveshape, as characterized by the half-wave potential and the Tafel slope as a function of the rate of mass transport and the cell geometry. Working surfaces are reported that allow the ready mechanistic interpretation of experimental data and the deduction of corresponding rate constants. Experiments are reported on the reduction of nitromethane in aqueous buffered solution ($7 < pH < 9$) at platinum electrodes that is thought to proceed via a heterogeneous ECEEE mechanism. Analysis of both waveshape and limiting current data confirm this mechanistic assignment, allowing the following appropriate kinetic parameters to be reported: heterogeneous rate constant, 0.26 ± 0.07 cm s^{-1}; and standard electrochemical rate constant, 0.13 ± 0.01 cm s^{-1}.

Introduction

Electrode reactions categorized by the Testa and Reinmuth notation[1] as ECE processes are defined by the following reaction scheme

$$\text{E step} \qquad A \pm e^- \rightarrow B$$

$$\text{C step} \qquad B \rightarrow C$$

$$\text{E step} \quad C \pm e^- \rightarrow \text{products}$$

in which it may be recognized that the C step may occur either homogeneously in a reaction layer close to the electrode or, alternatively, heterogeneously on the surface of the latter proceeding through the adsorption of B. Moreover, it has been recognized by Laviron[2] that discrimination between the two possibilities is far from straightforward, especially if the mechanistic determination is based exclusively on voltammetric (as opposed to spectroelectrochemical) procedures. In this context, we have discussed the application of hydrodynamic voltammetry in earlier papers[3,4] and, in particular, theoretically analyzed the mass transport and cell geometry dependence of the limiting current response at channel electrodes to establish the circumstances under which channel electrode voltammetry may or may not discriminate between the two limiting possibilities. It was established that the sought distinction can be made *in principle*, provided that current measurements can be undertaken over a sufficiently wide range of electrolyte flow rates.[4] However, in practice, unambiguous voltammetric characterization would be considerably assisted by the inclusion of the additional and essentially independent information resulting from the analysis of the voltammetric waveshape. Accordingly, in this paper we develop the theory of heterogeneous ECE processes at a channel electrode, paying attention to the effects of the chemical step on both the halfwave potential and the Tafel slope associated with the voltammogram. In particular, the latter will be shown to be a sensitive probe of the nature and magnitude of the coupled kinetics.

SCHEME 1

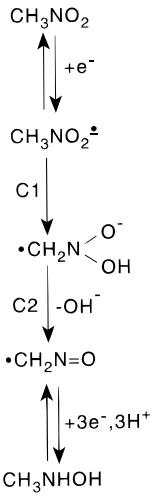

The methodology is applied to the reduction of nitromethane in aqueous solution, which is thought to involve the uptake of four electrons and four protons in addition to the cleavage of a N−O bond to produce methylhydroxylamine.[5−9] Despite the complexity of characterizing such a sequence, impedance voltammetry has been conspicuously effective at unravelling the key details of the mechanism for the case of mercury electrodes.[10−13] These details are summarized in Scheme 1 in which step C1 is heterogeneous but step C2 is homogeneous. For the cases of Hg/Cu[3] and Au/Hg[14] electrodes, step C1 was found to be rate limiting so that the reaction followed an ECEEE mechanism. On Au/Hg electrodes, a rate constant of 0.06 cm s^{-1} was inferred spectroelectrochemically[14] for step C1, which

S1089-5647(98)01731-3 CCC: $15.00 © 1998 American Chemical Society
Published on Web 07/31/1998

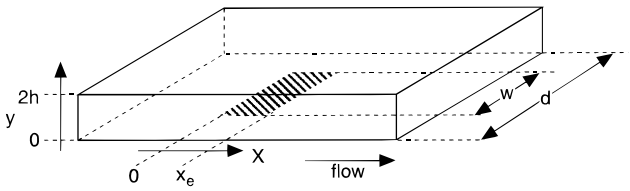

Figure 1. A schematic diagram defining the coordinate system used to charaterize a general channel electrode.

was close to that value deduced at pure mercury electrodes via impedance measurements.[13] The rate was found to be a little higher and also pH dependent for the case of Hg/Cu electrodes. In this paper, we examine the reduction at platinum electrodes to investigate further the sensitivity of the reaction to the chemical nature of the electrode material.

Theory

We consider a heterogeneous ECE mechanism where the chemical transformation

$$B \rightarrow C$$

occurs solely on the electrode surface with a rate constant k_{het}/cm s^{-1}. The convective-diffusion equations for a channel electrode describing the A and B distributions in time (t) and space (x,y) are

$$\frac{\partial[A]}{\partial t} = D_A\frac{\partial^2[A]}{\partial y^2} - \upsilon_x\frac{\partial[A]}{\partial x} \quad (1)$$

$$\frac{\partial[B]}{\partial t} = D_B\frac{\partial^2[B]}{\partial y^2} - \upsilon_x\frac{\partial[B]}{\partial x} \quad (2)$$

where D_A and D_B are the diffusion coefficients of species A and B. The Cartesian coordinates x and y are defined in Figure 1, which shows a generalized channel electrode in schematic form. The parameter υ_x is the solution velocity in the x-direction; the components in the y- and z-directions are zero. Given laminar flow conditions and that a sufficiently long lead-in length exists upstream of the electrodes to allow the full development of Poiseuille flow, then υ_x is parabolic

$$\upsilon_x = \upsilon_o\left(1 - \frac{(h-y)^2}{h^2}\right) \quad (3)$$

where h is the half-height of the cell and υ_o is the solution velocity at the center of the channel. Equations 1−3 assume that axial diffusion effects may be neglected; this assumption is valid provided the electrodes considered are not of microelectrode dimensions.[15]

The boundary conditions appropriate to the problem under investigation are as follows. Upstream of the electrode, the only species present is A at a concentration corresponding to its value in bulk solution

$$\text{all } y \qquad x < 0 \qquad [A] = [A]_{bulk} \qquad [B] = 0 \qquad [C] = 0 \quad (4)$$

At the electrode surface, the flux of A arriving must be balanced by the sum of the flux of B leaving and being converted into C

$$y = 0 \qquad 0 < x < x_e \qquad [A] = 0$$

$$D_A\frac{\partial[A]}{\partial y} = -D_B\frac{\partial[B]}{\partial y} + k_{het}[B] \quad (5)$$

Next, we assume that Butler−Volmer kinetics apply to the charge-transfer reaction at the electrode surface so that, considering a reduction process,

$$A + e^- \underset{k_b}{\overset{k_f}{\rightleftharpoons}} B$$

the electrochemical rate constants are given by

$$k_f = k_o\exp(-\alpha\theta) \quad (6)$$

$$k_b = k_o\exp(+\beta\theta) \quad (7)$$

where the dimensionless electrode potential is given by

$$\theta = (F/RT)(E - E^{\circ\prime}) \quad (8)$$

and E is the electrode potential, $E^{\circ\prime}$ is the formal potential of the A/B redox couple, and α and β are transfer coefficients. The arrival flux of A must match the net electrochemical conversion of A into B, so we can formulate another boundary condition applicable to the electrode surface

$$y = 0 \qquad 0 < x < x_e$$

$$D_A\frac{\partial[A]}{\partial y} = k_f[A]_{y=0} - k_b[B]_{y=0} \quad (9)$$

A final condition reflects the situation that for an ECE type reaction, all the C produced is destroyed electrochemically

$$y = 0 \qquad 0 < x < x_e$$

$$[C] = 0 \quad (10)$$

Finally at the wall of the cell, opposite to the electrode, a no-flux condition must operate

$$y = 2h \qquad all\ x$$

$$D_A\frac{\partial[A]}{\partial y} = D_B\frac{\partial[B]}{\partial y} = 0 \quad (11)$$

The set of mass transport eqs 1 and 2 can be solved under the boundary conditions just specified by direct application of an implicit finite-difference method previously optimized for the solution of mass transport problems in the channel electrode geometry.[16,17] References 15 and 18 relate a fully comprehensive account of the necessary detail, and the interested reader is directed to those sources. Programs were written in FORTRAN 77 and executed on a Silicon Graphics Origin. In typical simulations, 1000 grid points were used over the electrode length (x_e) and 500 over that fraction (ϕ) of the total channel depth ($2h$) which corresponds to no less than the maximum size of the diffusion layer thickness ($<\phi 2h$) so that the boundary conditions of eq 11 are applied at $y = \phi 2h$. Steady-state voltammograms were computed for various rate constants, k_{het} and k_o, by systematically changing the electrode potential θ for different channel electrode geometries; each voltammogram typically required ~20 s of CPU time (on an R10000 processor). The electrode currents flowing under the various conditions were evaluated using rectangular quadrature of the expression for ECE reactions

$$I(\theta) = Fw\int_0^{x_e}\left(D\frac{\partial[A]}{\partial y} + k_{het}[B]\right)_{y=0} dx \quad (12)$$

where w is the electrode width and x_e the electrode length

(Figure 1). For the case of ECEEE processes, the current expression is modified to

$$I(\theta) = Fw\int_0^{x_e}\left(D\frac{\partial[\mathrm{A}]}{\partial y} + 3k_{\mathrm{het}}[\mathrm{B}]\right)_{y=0} \mathrm{d}x \qquad (13)$$

Theoretical Results and Discussion

The model just described permits the simulation of the full current−voltage curve for any combination of chosen parameters (k_{het}, k_{o}, x_{e}, d, $2h$, and v_{o}). To simplify the presentation of our results, we note that almost all practical channel flow cells constructed for the pursuit of mechanistic insight operate so that the time taken to diffuse across the depth ($2h$) of the cell is significantly greater than that required to flow along the length of the electrode (x_{e}) so that[19,20]

$$\{(2h)^2/D\} \gg \{x_{\mathrm{e}}/v_{\mathrm{o}}\} \qquad (14)$$

This relationship has the consequence that any deviations from bulk concentrations induced by the electrode are confined to distances in the y-direction, which are small in comparison with the depth of the cell. This result permits, to high accuracy, the nonzero solution velocity component to be simplified according to the Lévêque approximation[21]

$$v_x \approx 2v_{\mathrm{o}}y/h \qquad (\text{for } y \approx 0) \qquad (15)$$

Second we assume that

$$D_{\mathrm{A}} = D_{\mathrm{B}} = D \qquad (16)$$

which is often an excellent assumption.[22] These two assumptions enable eqs 1 and 2 to be cast into dimensionless form[3,20] along with the boundary and other conditions in eqs 4−11. This readily permits the deduction that, subject to the validity of the two assumptions, the voltammetric response is controlled by two independent dimensionless parameters

$$K_{\mathrm{het}} = k_{\mathrm{het}}(hx_{\mathrm{e}}/2v_{\mathrm{o}}D^2)^{1/3} \qquad (17)$$

and

$$K_{\mathrm{o}} = k_0(hx_{\mathrm{e}}/2v_{\mathrm{o}}D^2)^{1/3} \qquad (18)$$

The quantities of interest characterizing the current−voltage waveshape are the halfwave potential, $E_{1/2}$, and the Tafel slope measured at this potential defined by

$$\left[\frac{\mathrm{d}E}{\mathrm{d}(\log_e[I^{-1} - I_{\mathrm{lim}}^{-1}])}\right]_{E=E_{1/2}} \qquad (19)$$

It is readily shown using standard arguments,[20] that the dimensionless halfwave potential

$$\theta_{1/2} = (F/RT)(E_{1/2} - E^{\circ\prime}) \qquad (20)$$

and Tafel slope

$$\left[\frac{\mathrm{d}\theta}{\mathrm{d}(\log_e[I^{-1} - I_{\mathrm{lim}}^{-1}])}\right]_{\theta=\theta_{1/2}} \qquad (21)$$

are functions solely of K_{het} and K_{o}. Accordingly, the results of our simulations may be summarized by working surfaces showing the variation of the two quantities of interest as functions of both K_{het} and K_{o}. Figure 2 shows the first of these quantities relating to the variation of $\theta_{1/2}$. It can be seen that for large enough values of K_{o} (corresponding to essentially electrochemically reversible conditions), the effect of the following chemical step is to shift the halfwave potential to less negative potentials than the formal potential ($E^{\circ\prime}$) in the case of a reduction. However as the value of K_{o} is decreased, the effect of the following kinetics (in comparison to the situation of no heterogeneous kinetics) becomes less and less. In particular, when the limit of essentially irreversible electrochemical kinetics ($K_{\mathrm{o}} \ll 1$) is reached, the observed halfwave potential is entirely insensitive to the surface-catalyzed loss of B and, as expected, occurs at (over)potentials negative of $E^{\circ\prime}$.

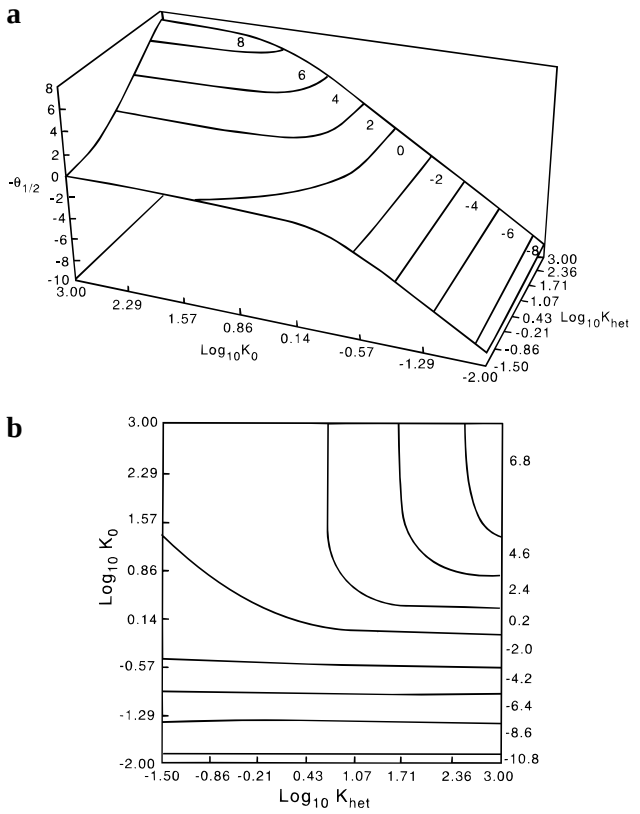

Figure 2. Working surface relating $\theta_{1/2}$ to the dimensionless parameters k_{het} and k_{o}: (a) a three-dimensional plot and (b) the corresponding contour plot.

Figure 3 shows the Tafel slope as a function of both K_{het} and K_{o}. At low values of K_{o}, larger values are seen, as expected for an electrochemically irreversible process at a channel electrode.[23] As K_{o} increases, however, the Tafel slope drops to that corresponding to an electrochemically reversible charge transfer and in this limit the Tafel slope is again independent of K_{o}. However, the value of K_{o} required to observe reversibility is larger in the presence of appreciable heterogeneous kinetics because of the loss of B through chemical reaction at the electrode surface. An implication of this result is that a redox couple, which has a k_{o} value sufficiently high to give rise to electrochemical reversibility under given mass transport conditions, can appear electrochemically irreversible if the electrode surface is highly efficient toward the decomposition of B.

Figures 2 and 3 together with the previously reported working curve relating n_{eff} (the effective number of electrons transferred under transport limited conditions) to K_{het} for a heterogeneous ECE mechanism, permit the quantitative analysis of experimental data for such processes. In particular we note that it should be possible to use limiting current and waveshape data

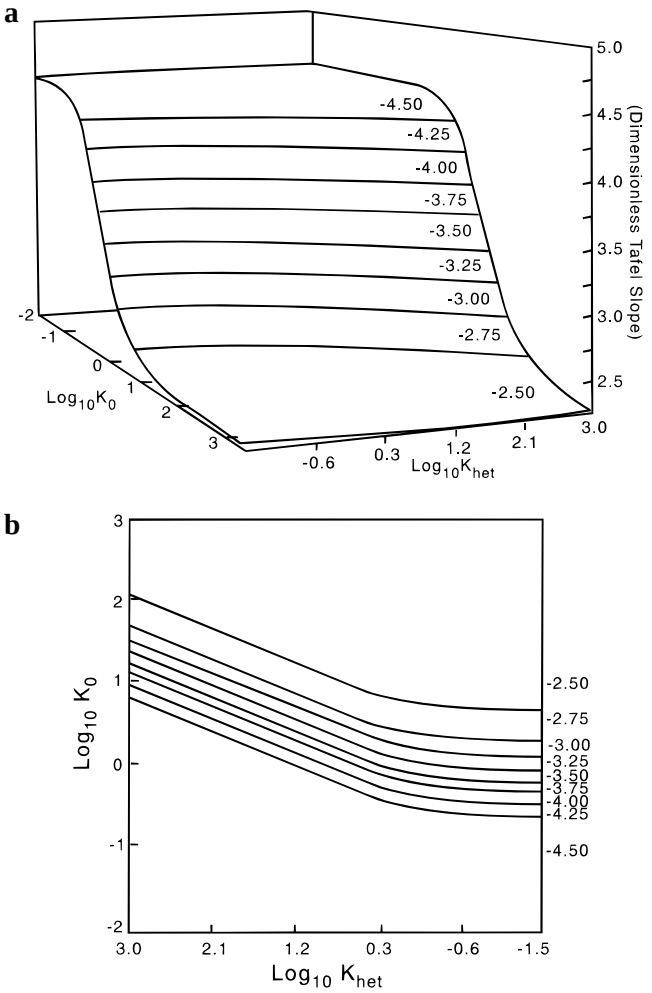

Figure 3. Working surface relating the dimensionless Tafel slope (eq 21) to the dimensionless parameters k_{het} and k_o: (a) A three-dimensional plot and (b) the corresponding contour plot.

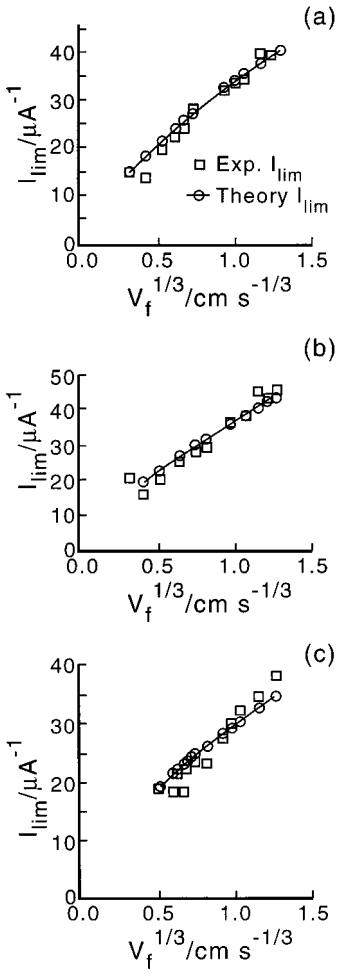

Figure 4. The variation of the transport-limited current with the electrolyte flow rate as measured (□) in buffered solutions of pH (a) 7.0, (b) 8.0, and (c) 9.0. The symbols (○) show the behavior simulated for an ECEEE mechanism using the following best-fit values of k_{het}: (a) 0.24, (b) 0.32, and (c) 0.16 cm s^{-1}.

to obtain mutually consistent values of k_{het} and that such a determination would provide a strong indication of the veracity of the mechanistic asignment.

In the following we apply the theoretical analysis just presented to the study of the reduction of nitromethane in aqueous solutions at platinum electrodes. In this context it should be noted that the working surfaces shown in Figures 2 and 3 apply equally to heterogeneous EC reactions and also to those mechanisms where any number of consecutive E steps follow the rate-determining C step, including the ECEEE case of interest presented next.

Experimental Section

A fast-flow channel electrode system was employed that could deliver solutions at flow rates of up to ~5 cm^3 s^{-1} through a flow cell constructed of silica with a cross-sectional area of 2 × 0.1 mm. Full details of the rig and operating procedures have been described earlier.[3,24] Platinum microband electrodes were fabricated by sealing a platinum foil strip (Goodfellow Metals, Cambridge, UK), 40 μm thick, between two glass rods followed by polishing in the manner reported elsewhere.[3] Precise determinations of the area of platinum exposed (40.6 μm × 0.094 cm) were obtained using either a scanning electron microscope or a Topometrix AFM. The working electrode potential was controlled through a conventional three-electrode potentiostat system with a platinum gauze counter electrode located downstream to prevent contamination by counter electrode electrolysis products. Potentials were measured relative to a platinum wire quasireference electrode. Measurements were made a temperature of 25 °C.

All solutions were made using Elgastat (High Wycombe, UK) UHQ grade water of resistivity 18 MΩ cm. Solutions of nitromethane (puriss, absolute, Fluka) were prepared immediately prior to the experiment and were buffered with buffer solutions based on either 0.2 M KH_2PO_4 (pH 7−7.5) or 0.2 M boric acid (pH 8−9). In all cases, the buffers were adjusted to the desired pH by addition of KOH solution and additionally contained 1.0 M KCl as supporting electrolyte. Solutions were thoroughly purged of oxygen before use with nitrogen, which had been presaturated by previous passage through an identical solution to that being deaerated.

Data analysis was conducted using a custom-written data analysis program (written in Microsoft Visual C++/MFC running under Windows 3.11, which allowed limiting currents and halfwave potentials to be measured from the voltammograms). Previous work[14] established a value of 2.0 × 10^{-5} cm^2 s^{-1} for the diffusion coefficient of nitromethane in aqueous solution, and this value was used in all modeling of experimental data.

Results and Discussion

Experiments were conducted on the reduction of nitromethane (~1.5 mM) in aqueous media (7.0 < pH < 9.0) using a 40-μm

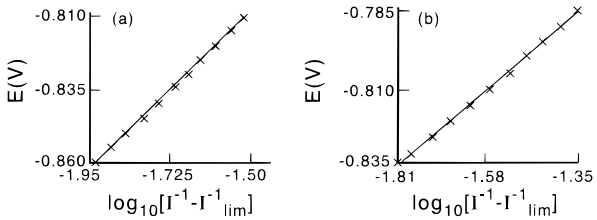

Figure 5. Typical Tafel plots recorded at flow rates of (a) 0.57 and (b) 0.079 $cm^3\ s^{-1}$ for a solution of pH 8.0.

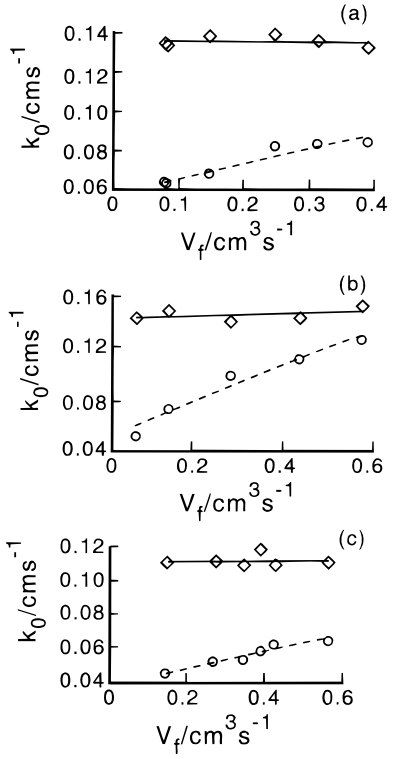

Figure 6. Variation of k_o with electrolyte flow rate as determined from measured Tafel slopes interpreted either in terms of a simple E process (- - -) or in terms of an ECEEE process (—) using the values of k_{het} determined for the appropriate pH via analysis of the transport-limited current.

platinum microband electrode in a fast-flow channel cell capable of volume flow rates (V_f) in the range 0.03−2.5 $cm^3\ s^{-1}$. The recorded voltammograms showed halfwave potentials in the range of −0.75 to −0.85 V (versus Pt pseudo-reference electrode), with no systematic change with pH. The variation with flow rate is considered later. In all cases, the transport-limited current was measured as a function of flow rate. Typical plots are shown in Figure 4 together with the best-fit behavior simulated for an ECEEE process with the theory previously developed[3] by optimizing the value of k_{het} in each case. It can be seen that the heterogeneous rate constants, k_{het}, lie between 0.16 and 0.36 cm s^{-1} and display no trend with pH. Note that the approximate linear dependence of the transport limited currents in Figure 4 with the cube root of the flow rate is strong evidence for a *heterogeneous* as opposed to homogeneous rate-determining chemical step.[3]

Next, to provide an independent check on the rate constant, Tafel slopes were measured for all the voltammetric waves by evaluating the expression in eq 21 by plotting E against log $[I^{-1} - I_{lim}{}^{-1}]$. Good linear plots were found in all cases, as typified by the data in Figure 5. However, when the Tafel slopes were analyzed in terms of a simple quasireversible E process using the relevant theory for a channel electrode,[23] the values of k_o determined showed a systematic variation with flow rate as shown in Figure 6. In contrast, when the analysis was conducted using the theory already reported for an ECEEE process and employing the pertinent values of k_{het} deduced from the transport-limited current data (Figure 4) for the relevant pH, the values of k_o were independent of flow rate and unchanging with flow rate over the range of the latter examined. These consistencies provide strong evidence that the mechanism is indeed of the ECEEE type and that the value of k_o is 0.13 ± 0.01 cm s^{-1}.

Finally, the variation of the halfwave potential with flow rate was considered. The values of k_{het} and k_o generated from the limiting current and Tafel slope analyses just given were used to simulate the flow rate dependence of the halfwave potential. The fits permitted the deduction of a mean value of −0.87 ± 0.05 V (versus Pt pseudo-reference electrode) for the formal potential, $E^{\circ\prime}$, of the $CH_3NO_2/[CH_3NO_2]^{\bullet-}$ redox couple.

Conclusions

Heterogeneous ECE type processes can be voltammetrically well characterized if both the flow rate dependence of the transport-limited current *and* the Tafel slope are examined in parallel. Values of the heterogeneous rate constant, k_{het}, and the standard electrochemical rate constant, k_o, can be deduced.

The reduction of nitromethane in aqueous media in the pH range 7.0−9.0 at platinum electrodes appears to follow a heterogeneous ECEEE mechanism with $k_o = 0.13 \pm 0.01$ cm s^{-1} and $k_{het} = 0.26 \pm 0.07$ cm s^{-1}. The overall mechanism is thus of the same type as determined at mercury electrodes[10−13] and at Hg/Cu[3] or Au/Hg[14] electrodes.

Acknowledgment. We thank the EC for a research training grant for FP under the Fourth Framework Program (contract no. ERB FMB ICT95 0219), the EPSRC for studentships for JAA and WJA, and Keble College, Oxford, for a Senior Scholarship for JAA.

References and Notes

(1) Testa, A. C.; Reinmuth, W. *Anal. Chem.* **1961**, *33*, 1320.
(2) Laviron, E. *J. Electroanal. Chem.* **1995**, *391*, 187.
(3) Aixill, W. J.; Alden, J. A.; Prieto, F.; Waller, G. A.; Compton, R. G.; Rueda, M. *J. Phys. Chem.* **1998**, *102*, 1515.
(4) Leslie, W.; Alden, J. A.; Compton, R. G. *J. Phys. Chem.* **1996**, *100*, 14130.
(5) Petru, F. *Collect. Czech. Chem. Commun.* **1947**, *12*, 620.
(6) Suzuki, M.; Elving, P. J. *Collect. Czech. Chem. Commun.* **1960**, *25*, 3202.
(7) Gavioli, G. B.; Grandi, G.; Andreolli, R. *Collect. Czech. Chem. Commun.* **1971**, *36*, 730.
(8) Wawzonek, S.; Tsung-Yuan, S. *J. Electrochem. Soc.* **1973**, *120*, 745.
(9) Guidelli, R.; Foresti, M. L. *J. Electroanal. Chem.* **1978**, *88*, 65.
(10) Rueda, M.; Sluyters-Rehbach, M.; Sluyters, J. H. *J. Electroanal. Chem.* **1989**, *261*, 23.
(11) Prieto, F.; Rueda, M.; Navarro, I.; Sluyters-Rehbach, M.; Sluyters, J. H. *J. Electroanal. Chem.* **1992**, *327*, 1.
(12) Prieto, F.; Rueda, M.; Navarro, I.; Sluyters-Rehbach, M.; Sluyters, J. H. *J. Electroanal. Chem.* **1996**, *405*, 1.
(13) Prieto, F.; Navarro, I.; Rueda, M. *J. Phys. Chem.* **1996**, *100*, 16346.
(14) Prieto, F.; Webster, R. D.; Alden, J. A.; Aixill, W. J.; Waller, G. A.; Compton, R. G.; Rueda, M. *J. Electroanal. Chem.* **1997**, *437*, 183.
(15) Alden, J. A.; Compton, R. G. *J. Electroanal. Chem.* **1996**, *404*, 27.
(16) Compton, R. G.; Pilkington, M. B. G.; Stearn, G. M. *J. Chem. Soc., Faraday Trans. I* **1988**, *84*, 2155.
(17) Fisher, A. C.; Compton, R. G. *J. Phys. Chem.* **1991**, *95*, 7538.
(18) Alden, J. A.; Compton, R. G. *J. Phys. Chem. B* **1997**, *101*, 8941.
(19) Compton, R. G.; Dryfe, R. A. W. *Prog. React. Kinet.* **1995**, *20*, 245.

(20) Cooper, J. A.; Compton; R. G. *Electroanalysis* **1998**, *10*, 141.
(21) Lévêque, M. A. *Ann. Mines Mem. Ser.* **1928**, *12/13*, 201.
(22) Wang, R. L.; Tam, K. Y.; Compton, R. G. *J. Electroanal. Chem.* **1997**, *434*, 105.
(23) Bidwell, M. J.; Alden, J. A.; Compton, R. G. *J. Electroanal. Chem.* **1996**, *417*, 119.
(24) Rees, N. V.; Dryfe, R. A. W.; Cooper, J. A.; Coles, B. A.; Compton, R. G. *J. Phys. Chem.* **1995**, *99*, 7096.